Available online at www.sciencedirect.com
SCIENCE DIRECT®

Flow Measurement and Instrumentation 16 (2005) 199–204

Flow Measurement and Instrumentation

www.elsevier.com/locate/flowmeasinst

Simulation study of the sensing field in electromagnetic tomography for two-phase flow measurement

Ze Liu[a,*], Min He[b], Hanliang Xiong[c]

[a] *Department of Automation, Beijing Jiaotong University, Beijing, PR China*
[b] *College of Engineering, Shanghai Maritime University, Shanghai, PR China*
[c] *Department of Automation, Tianjin University, Tianjin, PR China*

Received 10 October 2004; received in revised form 30 January 2005; accepted 15 February 2005

Abstract

The sensing field in the electromagnetic tomography (EMT) system has been studied based on a novel parallel excitation which uses a flexible circuit strips array. The principle of parallel excitation is analyzed. To find out the interaction between the excitation field and the object field which is produced by conductive and/or ferromagnetic materials in the measured space, both empty sensing field and object sensing field are simulated using the finite element method (FEM). The simulation result shows that this kind of parallel excitation is an effective solution of an EMT excitation system. A discussion of the dual mode imaging in EMT is also included.

Keywords: Process tomography; Electromagnetic tomography; Parallel excitation; FEM

1. Introduction

Electromagnetic tomography (EMT) can provide a reasonable way to measure the solid–gas flow and solid–liquid flow which contain magnetic material by reconstructing the images of the flow process. EMT, which was proposed ten years ago [1], is one of the electrical tomography technologies. It combines electromagnetic theory with computerized tomography technology. EMT also has another name: magnetic induction tomography (MIT) [2,3]. This technology can reconstruct the spatiotemporal distribution images of conductive and/or ferromagnetic materials by detecting the boundary magnetic flux density of the space being researched. In addition, the sensor of an EMT system has the advantages of being non-invasive, non-contacting and non-hazardous. So it can be used in the fields of industrial multiphase flow measurement, chemical abstraction, foreign material monitoring, geologic exploration and biomedical research. Furthermore, EMT can be used to develop advanced multi-phase flow measurement instruments, in combination with other electrical tomographies.

Three different electromagnetic tomography systems were reviewed by Peyton in 1996 [4]. The main difference of the three kinds of systems is the excitation mode. This paper focuses on the parallel excitation mode [5] and presents a kind of novel parallel excitation structure using a flexible circuit strips array. Based on this kind of novel excitation structure, the excitation sensing field is simulated using the finite element method (FEM). In order to investigate the interaction between the alternative excitation field and the material measured, the object fields to be simulated contain three test poles respectively, including a copper pole, a ferrite pole and a special pole, which are conductive and ferromagnetic. Finally, the characteristics of the dual mode imaging are discussed according to the simulation result.

2. Principle of parallel excitation

To construct a rotatable parallel excitation field, the current distributed around the measured pipe should be controlled according to the following rules. A parallel

* Corresponding author.
E-mail addresses: zliu@center.njtu.edu.cn (Z. Liu), hemin@eyou.com (M. He), hanliang@public.tpt.tj.cn (H. Xiong).

0955-5986/$ - see front matter
doi:10.1016/j.flowmeasinst.2005.02.008

Nomenclature

$\mathbf{B}$	magnetic flux density, T
I	excitation current, A
I_D	excitation current of point D in Eq. (2.5), A
I_E	excitation current of point E in Eq. (2.5), A
K_0	surface current density, A/m
R	radius, mm
σ	conductivity, S/m
μ_r	relative permeability

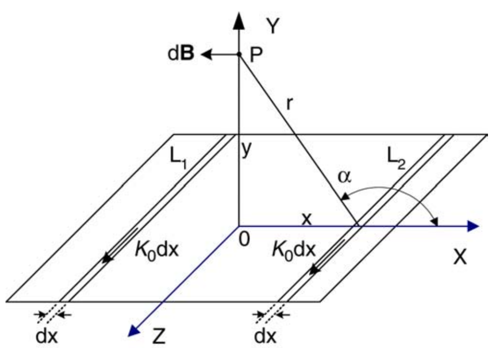

Fig. 1. Magnetic flux density of an infinite current board.

magnetic field can be generated by using an infinite current board. Fig. 1 shows the theory model of the magnetic flux density generated by an infinite current board. Considering an arbitrary point P above the infinite current board, its magnetic flux density d$\mathbf{B}$ which is generated by the two current lines L_1 and L_2 distributed on the XOZ plane, is enhanced in the X direction and counteracted in the Y direction. So the magnetic flux density distribution beside the infinite current board can be calculated from Eq. (2.1):

$$\begin{aligned}\mathbf{B} &= B_X\mathbf{i} = \left[-\int_{-\infty}^{\infty}\frac{\mu K_0\sin\alpha}{2\pi(x^2+y^2)^{1/2}}\mathrm{d}x\right]\mathbf{i}\\ &= \left[-\frac{\mu K_0 y}{2\pi}\int_{-\infty}^{+\infty}\frac{\mathrm{d}x}{x^2+y^2}\right]\mathbf{i}\\ &= \left[-\frac{\mu K_0}{2\pi}\arctan\frac{x}{y}\Big|_{-\infty}^{+\infty}\right]\mathbf{i}\\ &= \begin{cases}-\dfrac{\mu K_0}{2}\mathbf{i}, & y>0\\ +\dfrac{\mu K_0}{2}\mathbf{i}, & y<0,\end{cases}\end{aligned} \tag{2.1}$$

where $\mathbf{B}$ is the magnetic flux density generated by the infinite current board. In Eq. (2.1), B_X is the magnetic flux density in the X direction; K_0 is the surface current density of the infinite board with unit thickness. Eq. (2.1) shows that the magnetic flux densities (above and below the board) are equal in magnitude and opposite in direction.

If a parallel infinite current board, in which the current direction is opposite, is fixed above the former board, the magnetic flux density distributions of these two boards will be as shown in Fig. 2. So the magnetic flux density generated by boards I and II can be induced by Eq. (2.1) and be described by Eqs. (2.2) and (2.3):

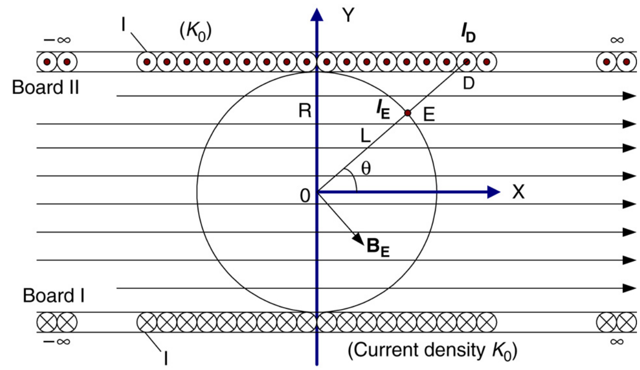

Fig. 2. Magnetic flux density of two infinite current boards.

$$\mathbf{B}_\mathrm{I} = \begin{cases}+\dfrac{\mu K_0}{2}\mathbf{i}, & y>-R\\ -\dfrac{\mu K_0}{2}\mathbf{i}, & y<-R\end{cases} \tag{2.2}$$

$$\mathbf{B}_\mathrm{II} = \begin{cases}+\dfrac{\mu K_0}{2}\mathbf{i}, & y<R\\ -\dfrac{\mu K_0}{2}\mathbf{i}, & y>R.\end{cases} \tag{2.3}$$

Combining Eqs. (2.2) and (2.3) and using the superposition principle, the magnetic flux density between boards I and II can be obtained by Eq. (2.4):

$$\mathbf{B} = +\mu K_0\mathbf{i}, \qquad -R<y<R. \tag{2.4}$$

As shown in Fig. 2, suppose the current distributed along the circle between boards I and II can generate the same magnetic flux density in the center as that of the two parallel boards. The magnetic flux density generated by I_D and I_E should be equal in the center of the circle. They are shown in Eq. (2.5):

$$B_D = \frac{\mu I_D}{2\pi L} \qquad B_E = \frac{\mu I_E}{2\pi R}. \tag{2.5}$$

So the excitation current of point E, I_E, can be calculated by Eq. (2.6):

$$I_E = I_D\sin\theta. \tag{2.6}$$

Furthermore, by using the integral method along the current distribution path and the Biot–Savart law, the magnetic flux density of an arbitrary point among the circle excited by the current distribution along the circle can be proved to be equal to that excited by the two infinite boards. So, if the excitation current along the circle satisfies Eq. (2.6), then the magnetic flux density among the circle will be parallel and even [5]. Moreover, the excitation field rotation can be realized by controlling the distribution of the excitation currents in the flexible circuit strips array along the excitation circle.

3. Sensing field simulation of a novel parallel excitation

3.1. Realization of a parallel excitation

In the actual exciting system of EMT, the distribution of exciting current along the excitation layer cannot be set continuously. A novel excitation structure using a flexible current strips array has been designed and applied in the experimental system. The system can reconstruct initial images of test poles [6]. Its excitation system uses 32 flexible current strips which are arranged uniformly around the excitation circle. The current distribution on each strip is given by Eq. (3.1):

$$I_i = I \sin(\varphi_i - p\theta_0)\sin(\omega t + \phi_0), \quad (3.1)$$

where i denotes the excitation strip number, p is the excitation projection sequence number, φ_i is the angle of excitation strip i, and θ_0 is the angle difference of the two adjacent excitation projections. $I \cdot \sin(\omega t + \phi_0)$ is the notation of the excitation signal. The maximum current of the strips is 10 mA. Compared with the parallel excitation implementation using two orthogonal excitation coils [4,5], the advantage of this kind of excitation is that the exciting current of every exciting strip around the circle can be controlled flexibly and independently.

3.2. Simulation of the empty excitation field

Bias error will appear if the parallel excitation is constructed by using finite flexible circuit strips because the strips cannot be fixed infinitely. For analyzing the excitation sensing field of the nonideal excitation structure, the magnetic flux density distribution is simulated by using an FEM based on the actual sensor structure. The simulation conditions are as follows. The radius of the measured pipe is 35 mm. The material of the pipe is organic glasses. The radius of electromagnetic shield layer is 60 mm. In the actual EMT system, the electromagnetic shield layer is made up of ferrite rings and a permalloy cylinder. In the simulation model, the magnetic vector potential of the shield layer is constrained as equal to emulate the condition of the actual structure. The radius of the excitation layer is 55 mm. 32 flexible excitation strips are arranged uniformly around the excitation layer. The excitation currents on the strips are distributed around the pipe according to Eq. (3.1). Under these conditions, the simulated magnetic flux line distribution of the empty measured pipe is shown in Fig. 3.

In Fig. 3, the outer layer is the electromagnetic shield layer. The inner layers are the excitation layer, detection layer, outer wall of the measured pipe and inner wall of measured pipe in turn. Fig. 3 shows that the magnetic flux lines in the measured pipe are parallel and even. Fig. 4 is the simulated magnetic flux density distribution of the empty field. The X–Y plane denotes the cross section of the sensor; the Z-axis is the magnitude of the magnetic flux density. As shown in Fig. 4, the magnetic flux densities in the cross

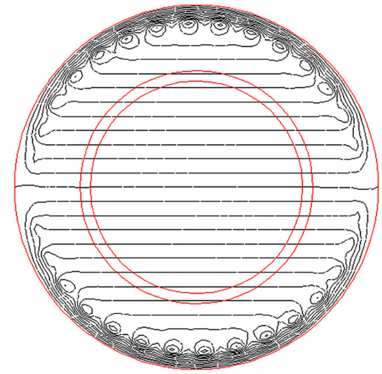

Fig. 3. Distribution of magnetic flux lines in empty field.

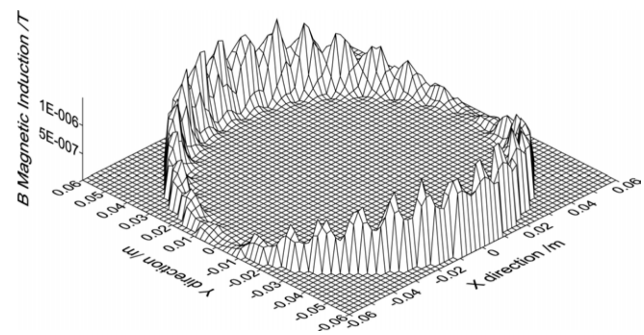

Fig. 4. Distribution of magnetic flux density in empty field.

section of the measured pipe ($R = 35$ mm) are equal, and its magnitude is 1.0985×10^{-7} T. According to the former theoretical analysis, the magnetic flux density in the cross section of the pipe can be calculated; it is 1.01467×10^{-7} T. So the simulation result of the sensing field is similar to the result of the theoretical analysis.

3.3. Simulation of sensing fields

Sensing fields of detectors in the parallel excitation EMT system are simulated by electromagnetic FEM. Sensing field diagrams of detectors are shown as Fig. 5 partly. The excitation direction is the first projection. The sensing fields of detectors in other directions are similar to these. It shows that as the position to detectors goes nearer the sensitivity get higher. The last sensing field in Fig. 5 is the general sensing field of the total eight detectors. It is the sum of the eight detectors' sensing fields. As shown in Fig. 5, the sensitivity in the center is the lowest. And the detectors, which are vertical to the excitation direction, have higher sensitivity than parallel ones. This is the individual feature of a parallel excitation system.

4. Simulation of interaction between excitation field and object

To analyze the interaction between the excitation field and the measured object, the sensing fields with conductive

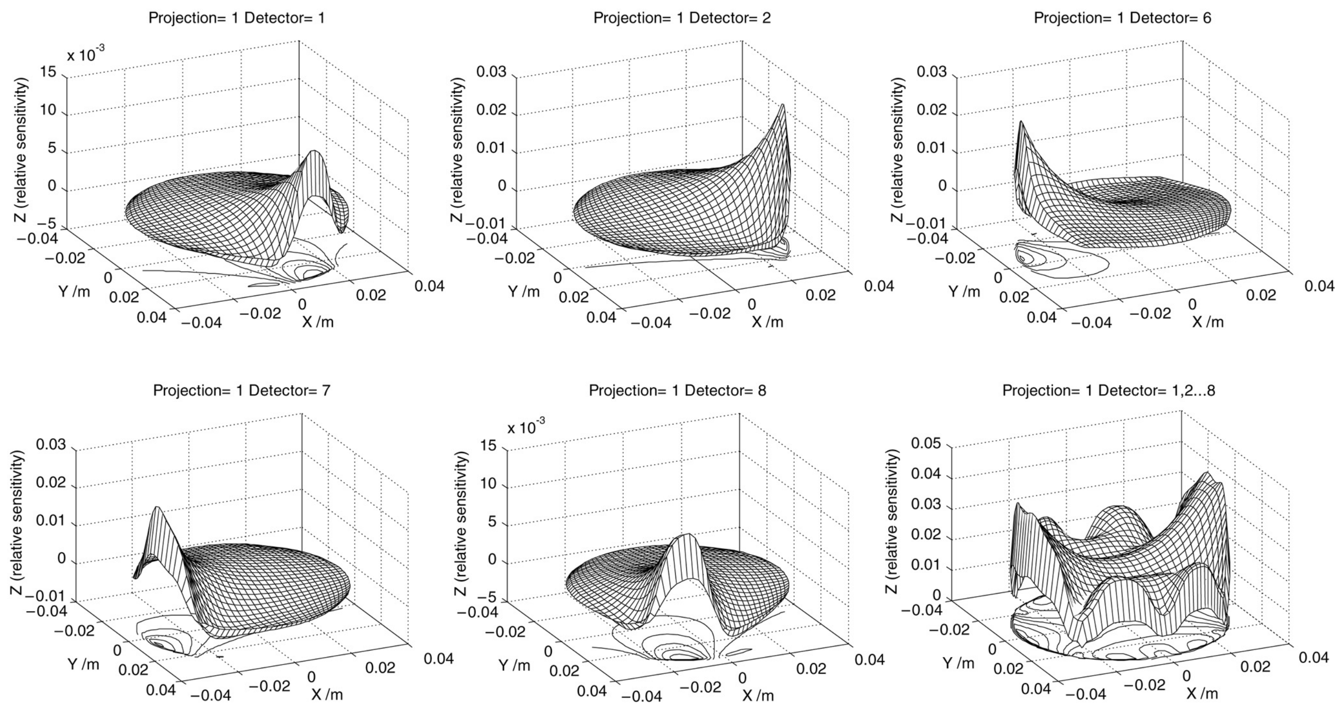

Fig. 5. Sensing fields of detectors in first projection.

and/or ferromagnetic object are simulated by using the FEM. Test objects are as follows: a copper pole whose conductivity is 5.87×10^7 S/m, a ferrite pole whose relative permeability is 200, and a special pole whose conductivity is 5.87×10^7 S/m and relative permeability is 200. The radius of these poles is 10 mm. The frequency of the excitation signals is 200 kHz. The simulated distributions of magnetic flux lines and magnetic flux density are shown in Fig. 6. Fig. 6(a) shows the distributions of magnetic flux lines and flux density distribution with the copper pole in the center of the measured pipe, (b) with the ferrite pole, (c) with the special pole. In the graphs in the right column, the X–Y plane is the cross section of the measured pipe and the Z-axis is the magnitude of the magnetic flux density.

The simulation result shows that the conductive object excludes the magnetic flux lines, but the ferromagnetic object attracts the magnetic flux lines. In Fig. 6(c), the special pole generates a complex interaction with the excitation field.

To analyze the distributions more obviously, magnetic flux density distributions along X-axis, Y-axis and the detection layer ($R = 38.4$ mm) are shown in Fig. 7. The four lines in the graphs denote the magnetic flux density distributions of the empty field, field with the copper pole, field with the ferrite pole, and field with the special pole. The line styles of the three graphs are shown in the legend of graph 7(c). The X-axis is the direction of excitation projection. As shown in (a) and (b), ferromagnetic material evidently reinforces the magnetic flux density, and in its inner area the magnetic flux density reaches a maximum value; but conductive material weakens the magnetic flux density, and in its inner area the magnetic flux density almost decreases to zero. The result coincides with the theoretical analysis that a conductive object in the alternative excitation field can generate an eddy current and a ferromagnetic object can be magnetized. The direction of magnetic flux density generated by the eddy current is opposite to the excitation direction, whereas the direction of magnetic flux density generated by a ferromagnetic material is the same as the excitation direction. Fig. 7 also shows that the magnetic flux densities modulated by the conductive and ferromagnetic material are coupled to each other. Obviously this kind of coupling is nonlinear.

5. Conclusion and discussion

Parallel excitation in an EMT system can be obtained by using alternative excitation currents which are distributed along the excitation layer outside the measured pipe. By controlling the current distribution, the magnetic excitation projection can be rotated. A novel structure of parallel excitation, which uses a flexible current strip array, is presented and its sensing field is simulated based on an actual sensor system. The simulation results show that this kind of excitation structure can generate an even and parallel magnetic excitation field in the measured pipe. Conductive and ferromagnetic materials have evident interaction with the excitation field. So this kind of excitation structure can be used to reconstruct images of conductive

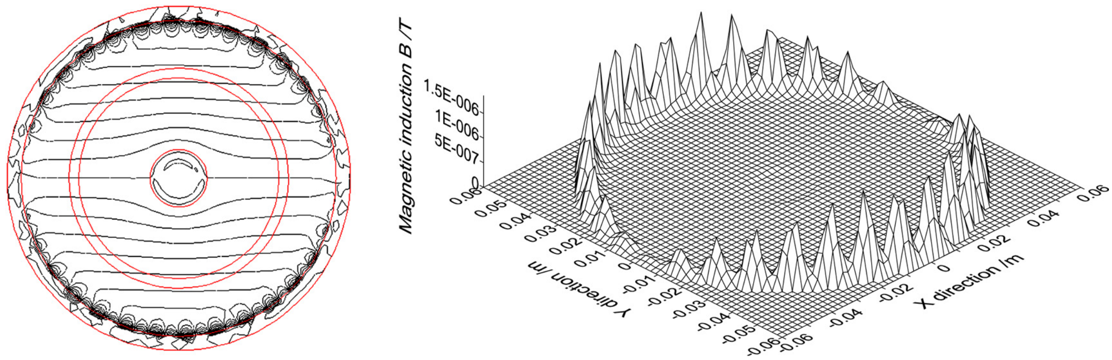

(a) Copper pole ($R = 10$ mm, $\sigma = 5.87 \times 10^7$ S/m) in the center of the pipe.

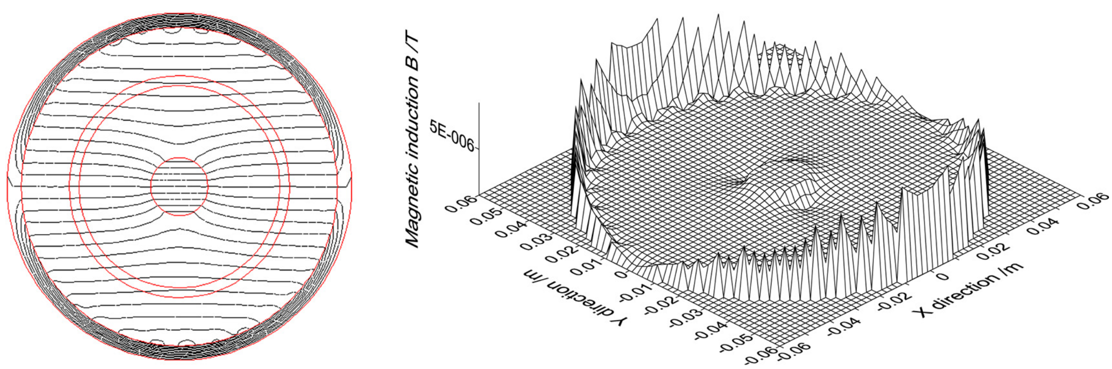

(b) Ferrite pole ($R = 10$ mm, $\mu_r = 200$) in the center of the pipe.

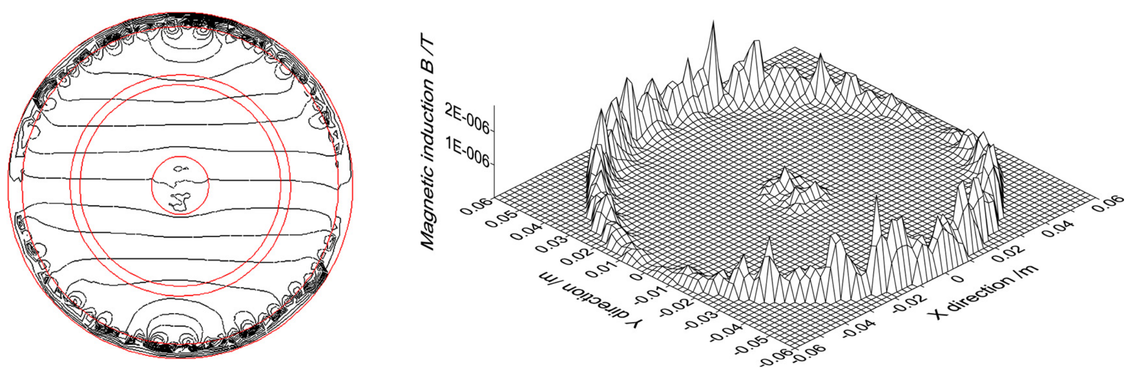

(c) Special pole ($R = 10$ mm, $\sigma = 5.87 \times 10^7$ S/m, $\mu_r = 200$) in the center of the pipe.

Fig. 6. Distribution of magnetic flux lines and flux density of a parallel excitation field with objects.

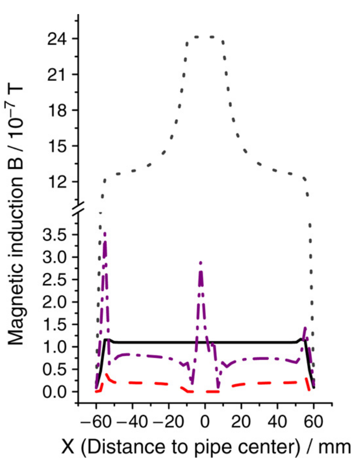

(a) Along the X-axis.

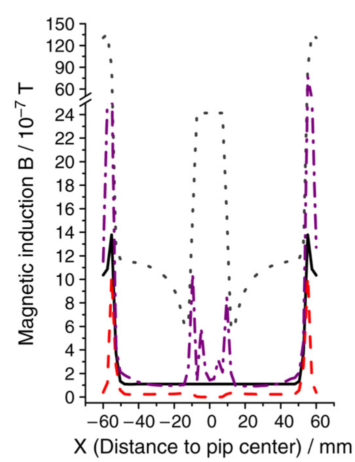

(b) Along the Y-axis.

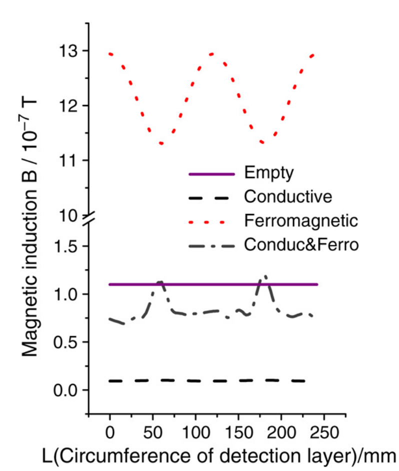

(c) Along a circle of the detection layer.

Fig. 7. Magnetic flux density distribution in a parallel excitation field along different paths.

or ferromagnetic materials. But investigations are still needed for reconstructing images of both conductive and ferromagnetic material at the same time. The reason is that the interaction of conductive and ferromagnetic materials is coupled to each other nonlinearly. This phenomenon brings a challenge to the realization of dual mode imaging in an EMT system. Some technologies, such as complex signal excitation and demodulation, sensitivity decoupling, and multi-frequency excitation, may provide solutions to these difficulties.

Acknowledgements

The authors would like to thank the National Natural Science Foundation of the People's Republic of China for support through grant number 60302011.

References

[1] S. AL-Zeibak, N.H. Saunders, A feasible study of in vivo electromagnetic imaging, Phys. Med. Biol. 38 (1993) 151–160.
[2] A. Korjenevsky, V. Cherepenin, S. Sapetsky, Magnetic induction tomography: experimental realization, Physiol. Meas. 21 (2000) 89–94.
[3] S. Watson, R.J. Williams, W. Gough, A. Morris, H. Griffiths, Phase measurement in biomedical magnetic induction tomography, in: 2nd World Congress on Industrial Process Tomography, Hanover, Germany, 29th–31st August 2001.
[4] A.J. Peyton, Z.Z. Yu, G. Lyon, S. Al-Zeibak, J. Ferreira, J. Velez, F. Linhares, A.R. Borges, H.L. Xiong, N.H. Saunders, M.S. Beck, Overview of electromagnetic inductance tomography: description of three different systems, Meas. Sci. Technol. 73 (1996) 261–271.
[5] Z.Z. Yu, A.J. Peyton, M.S. Beck, Electromagnetic Tomography (EMT): Part I: Design of sensor and electronics for a system with a parallel excitation field, European concerted action on process tomography, Portugal, April 1994, pp. 147–154.
[6] Ze Liu, Min He, Ling-an Xu, Hanliang Xiong, Multi-mode excitation electromagnetic tomography system, Chinese J. Sci. Instrum. 22 (6) (2001) 614–621.